DISCRETE AND CONTINUOUS
DYNAMICAL SYSTEMS SERIES B
Volume **12**, Number **2**, September **2009**

doi:10.3934/dcdsb.2009.12.495

pp. **495–511**

A METAPOPULATION MODEL WITH LOCAL COMPETITIONS

Dashun Xu

Department of Mathematics
Southern Illinois University
Carbondale, IL 62901, USA

Zhilan Feng

Department of Mathematics
Purdue University
West Lafayette, IN 47907, USA

Abstract. A metapopulation model with explicit local dynamics is studied. Unlike many patch-based metapopulation models which assume that the local population within each patch is at its equilibrium, our model incorporates population changes in local patches that interact with metapopulation dynamics. The model keeps track of the fractions of patches that have species 1 only, species 2 only, or both species. For patches with both species, the Lotka-Volterra type of competition is assumed. It is shown that when the local dynamics is coupled with the metapopulation dynamics the model outcomes can be very different comparing with metapopulation models that do not explicitly include local population dynamics. The analysis of the coupled system is carried out by using techniques in singular perturbation theory.

1. **Introduction.** In 1969, Levins considered the following single-species metapopulation model which assumes that changes in patch occupancy are functions solely of colonization rates of empty patches (c) and extinction rates of occupied patches (e):

$$\frac{dp}{dt} = cp(1-p) - ep, \tag{1}$$

where p denotes the proportion of the occupied patches. This simple model captures the basic fact that species persistence depends on the balance between local extinction and recolonization. Based on this framework, metapopulation models have been used extensively to analyze the dynamics of species in fragmented landscapes and to understand the potential implication of habitat fragmentation. For example, [1, 7, 9, 10, 11, 22] studied the dynamics of single species in a network of habitat fragments while [4, 15, 16, 17, 20] investigated the interaction of multispecies. Just like model (1), all these works fail to account for the local population dynamics. The colonization rate c in model (1) is directly related to migration rates. For species with high emigration rates, the lack of incorporation of local dynamics may lead to biased predictions (see, for example, [8]).

2000 *Mathematics Subject Classification.* Primary: 92B05; Secondary: 34A34.

Key words and phrases. Metapopulation models; Local population dynamics; Competition; Coexistence.

This research is supported in part by the NSF grants DMS-0719783 to DX and DMS-0719697 to ZF.

Hanski and Zhang [6] first incorporated the local dynamics into Levins' model (1) to study a single species with high migration rates and demonstrated that models with local dynamics can provide insights into conditions for metapopulation persistence that can not be obtained from simple patch models. Let N be the average size of existing local populations and p be the fraction of occupied habitat patches. The model ([6]) with a local dynamics is given as follows:

$$\begin{aligned} N' &= rN(1-\tfrac{N}{K}) - mN + \alpha mNp, \\ p' &= \beta\alpha mNp(1-p) - ep, \end{aligned} \tag{2}$$

where r is the average growth rate due to local births and deaths, m is the per capita emigration rate, K is the average local carrying capacity, α is the fraction of migrating individuals that survived and landed a new patch, β is the probability that an arriving individual gives rise to a new local population in an empty patch, and e is the extinction rate of local populations.

The model (2) assumes that local populations are affected by migrations and that changes in the metapulation size p occurs at a much slower time scale than those in the local popopulation size N because of low colonization rate [6]. For a certain range of parameter values, the model predicts an alternative stable equilibrium and qualitatively different model behaviors from those of model (1). From model (2) it was concluded that species with intermediate migration rates persist best in a fragmented landscape, which is different from what have been suggested by simple patch models.

Under the same assumptions of model (2), Feng et al ([2, 3]) incorporated Lotka-Volterra type of competition into model (2) and weak competitions of two species were studied through the following model

$$\begin{aligned} N_i' &= r_iN_i(1-\tfrac{N_i}{K_i} - a_{ji}\tfrac{N_j}{K_i}) - m_iN_i + \alpha_i m_i N_i p_i, \\ p_i' &= \beta_i\alpha_i m_i N_i p_i(1-p_i) - e_i p_i, \quad 1 \le i \ne j \le 2, \end{aligned} \tag{3}$$

where N_i denotes the typical population size of species i; p_i denotes the fraction of habitat patches occupied by species i (notice that $p_1 + p_2$ may be greater than one here); r_i is the average per capita growth rate due to local births and deaths; a_{ij} model the intensities of the local competition between two species, which are assumed to be weak, i.e., $a_{ij} < 1$; m_i is the per capita emigration rate; K_i is the average carrying capacity of species i; α_i describes migration costs, the fraction of migrating individuals that survived and reached a new patch; β_i is the probability that an arriving individual gives rise to a new local population in an empty patch; e_i is the extinction rate of local populations, which is assumed to be independent of N_i. All parameters and their definitions are listed in Table 1. The generalized model (3) displays much richer dynamics, varying from a unique global interior attractor to multiple interior equilibria as well as bistable phenomena (two stable, biologically feasible equilibria). These results imply that failure to account for competition interactions within local patches may lead to biased predictions regarding persistence of species.

For simplification purposes, the model (3) assumes that the competition between the two species occur on all patches that are occupied by either one or two species. In this paper, we modify this by assuming that the competition between the two species occur only on patches that are occupied by both species and we explicitly model the changes in the fraction of patches occupied by both species. Obviously, this is a more realistic assumption, although the model becomes more complex and the analysis will be more difficult. Following the same approach as in [2, 3, 6] which takes the

TABLE 1. Definitions of parameters ($i, j = 1, 2$).

N_i	the typical population size of species i on a habitat patch.
r_i	the average per capita growth rate due to local births and deaths.
a_{ij}	the intensities of the local competition between two species.
K_i	the average carrying capacity of species i.
α_i	the fraction of migrating individuals that survived and reached a new patch.
β_i	the probability that an arriving individual gives rise to a new local population in an empty patch.
e_i	the extinction rate of local populations.
σ_{ij}	the reduction in the colonization rate of species i due to the competition effect from species j.
ε_{ij}	the addition to the extinction rate of species i within doubly occupied patches via interaction with species j.

advantage of the fact that local dynamics occurs on a slower time scale than changes in patch occupancy, we can study the local (fast) and regional (slow) dynamics separately. Our analysis of slow dynamics shows that the model admits up to three interior equilibria, one of which is stable. Bistability may occur between either two boundary equilibria (representing only one species existing regionally) or boundary and interior equilibria. Moreover, the new model is capable of producing triple stable equilibria among boundary and interior equilibria. The bifurcation analysis shows that the system has a saddle-node bifurcation point of interior equilibria which lies in the parameter region where a boundary equilibrium is stable. This may have an important ecological implication for the metapopulation dynamics. That is, if the coexistence state is near the bifurcation point slight perturbations of environmental conditions may cause a dramatic alteration of the metapopulation in which the coexistence state may collapse into a state with only one species present.

2. **The model.** Let p_0, p_1, p_2 and p_3 be the fractions of empty habitat patches, patches occupied by species 1 only , species 2 only and both species, respectively. Then, $p_0 + p_1 + p_2 + p_3 = 1$. Let N_i $(i = 1, 2)$ denote the typical population size of species i existing on a habitat patch. Assume that the competition of two species on doubly-occupied patches is of the Lotka-Volterra type. In addition, we restrict our attention to the case in which the system does not stabilize at the metapopulation extinction state. Our model which couples the metapopulation changes and local population dynamics is as follows:

$$\begin{aligned}
N_1' &= r_1 N_1(1 - \tfrac{N_1}{K_1} - a_{21} p_3 \tfrac{N_2}{K_1}) - m_1 N_1 + \alpha_1 m_1 y_1 N_1, \\
N_2' &= r_2 N_2(1 - \tfrac{N_2}{K_2} - a_{12} p_3 \tfrac{N_1}{K_2}) - m_2 N_2 + \alpha_2 m_2 y_2 N_2, \\
p_1' &= \beta_1 \alpha_1 m_1 N_1 y_1 p_0 - e_1 p_1 - \sigma_{21}\beta_2 \alpha_2 m_2 N_2 y_2 p_1 + (e_2 + \varepsilon_{21}) p_3, \\
p_2' &= \beta_2 \alpha_2 m_2 N_2 y_2 p_0 - e_2 p_2 - \sigma_{12}\beta_1 \alpha_1 m_1 N_1 y_1 p_2 + (e_1 + \varepsilon_{12}) p_3, \\
p_3' &= \sigma_{12}\beta_1 \alpha_1 m_1 N_1 y_1 p_2 + \sigma_{21}\beta_2 \alpha_2 m_2 N_2 y_2 p_1 - (e_1 + \varepsilon_{12} + e_2 + \varepsilon_{21}) p_3,
\end{aligned} \tag{4}$$

where $y_1 = p_1 + p_3$, $y_2 = p_2 + p_3$. The parameter $\sigma_{ij} \in (0, 1]$ models the reduction in the colonization rate of species i due to the competition effect from species j; ε_{ij} is the addition to the extinction rate of species i within doubly occupied patches via interaction with species j [12]. All other parameters here admit the same meanings as in model (3) (see Table 1). However, the emigration rate m_i here is assumed to

be less than the birth rate r_i. In fact, as will be seen later, to ensure the persistence of a metapopulation, the emigration rate needs to be less than a certain critical value so that the size of local populations is large enough to generate emigration and recolonization [6]. Some of the model structures in (4) are similar to that considered in Taneyhill [21].

3. **The fast and slow systems.** Since changes in local population sizes occur at a faster time scale than changes in patch occupancy, the rate of patch creation by one migrating individual, $\beta_i\alpha_i m_i$, the rate of patch extinction, e_i, and the additional extinction rate ε_{ij} are much smaller than those related to local population dynamics. This allows us to study the system (4) by considering the two processes separately using tools in dynamical systems theory as illustrated below. Assume that

$$\beta_i = \epsilon\bar{\beta}_i,\ e_i = \epsilon\bar{e}_i,\ \varepsilon_{ij} = \epsilon\bar{\varepsilon}_{ij},\quad \epsilon > 0,$$

where ϵ is a small parameter. Then system (4) takes the following form:

$$\begin{aligned} N_i' &= N_i F_i(N_1, N_2, p_1, p_2, p_3),\\ p_i' &= \epsilon G_i(N_1, N_2, p_1, p_2, p_3),\quad i = 1, 2,\\ p_3' &= \epsilon G_3(N_1, N_2, p_1, p_2, p_3), \end{aligned} \tag{5}$$

where

$$\begin{aligned} &F_i(N_1, N_2, p_1, p_2, p_3) = r_i(1 - \tfrac{N_i}{K_i} - a_{ji}p_3\tfrac{N_j}{K_i}) - m_i + \alpha_i m_i y_i,\\ &G_i(N_1, N_2, p_1, p_2, p_3) = b_i N_i y_i p_0 - \bar{e}_i p_i - \sigma_{ji} b_j N_j y_j p_i + E_j p_3,\quad 1 \le i \ne j \le 2,\\ &G_3(N_1, N_2, p_1, p_2, p_3) = \sigma_{12} b_1 N_1 y_1 p_2 + \sigma_{21} b_2 N_2 y_2 p_1 - (E_1 + E_2)p_3, \end{aligned}$$

and $b_i = \bar{\beta}_i\alpha_i m_i$, $E_i = \bar{e}_i + \bar{\varepsilon}_{ij}$.

Using techniques in singular perturbation theory, we can analyze (5) by studying the corresponding fast and slow systems. Setting $\epsilon = 0$, the fast dynamics of (5) are given by

$$N_i' = N_i F_i(N_1, N_2, p_1, p_2, p_3),\ i = 1, 2. \tag{6}$$

Setting the right sides of (6) equal to zero, we can obtain the unique equilibrium $N^* = (N_1^*, N_2^*)$ (regarding p_1, p_2, p_3 as parameters in this stage), which is characterized by

$$\begin{aligned} N_1^* &= \tfrac{1}{1 - a_{12}a_{21}p_3^2}[k_{10} + k_{11}y_1 - (k_{20} + k_{21}y_2)a_{21}p_3],\\ N_2^* &= \tfrac{1}{1 - a_{12}a_{21}p_3^2}[k_{20} + k_{21}y_2 - (k_{10} + k_{11}y_1)a_{12}p_3], \end{aligned} \tag{7}$$

where

$$k_{i0} = K_i(1 - m_i/r_i),\quad k_{i1} = K_i\alpha_i m_i/r_i. \tag{8}$$

We are only concerned with the case where the coexistence of two species is possible, which is expected if and only if the competition intensity is weak, i.e, $a_{12}, a_{21} < 1$. For biological feasible scenarios, parameter values are chosen such that $N_i^* \ge 0$.

Direct calculations show that the Jacobian of system (6) at the equilibrium N^* admits two negative eigenvalues. Therefore, N^* is locally asymptotically stable. That is, on the fast time scale, all positive solutions of (5) are hyperbolically asymptotic to the equilibrium N^*. Rescaling the time by letting $\tau = t/\epsilon$, and denoting $d/d\tau$ by "$'$", we obtain the slow system which governs the dynamics on the slow manifold N^*:

$$p_i' = G_i(N_1^*, N_2^*, p_1, p_2, p_3),\ i = 1, 2, 3. \tag{9}$$

Since the long-term behavior of the system (5) is actually governed by the slow system (9) for small ϵ, we next focus on the dynamics of (9). It is worthwhile to point out that the system (9) is formally the same as Slatkin's model [19] and its

variation models in [4, 18, 21] except that here the system involves in the local dynamics. Therefore, the effect of the local dynamics on the regional dynamics which was studies in [4, 18, 19, 21] can be examined by studying system (9).

It is very difficult to solve the slow system (9) for interior equilibria. Nonetheless, the stability of the boundary equilibria can be obtained. Although the probability of simultaneous local extinctions of the two species can be biologically assumed to be zero, the investigation of stability of the trivial solution $Q_0 = (0, 0, 0)$ provides useful information for the study of other possible boundary equilibria. The Jacobian of the system (9) at Q_0 takes the from of

$$\begin{pmatrix} \delta_1 & 0 & b_1k_{10} + E_2 \\ 0 & \delta_2 & b_2k_{20} + E_1 \\ 0 & 0 & -E_1 - E_2 \end{pmatrix},$$

where

$$\delta_i = b_ik_{i0} - \bar{e_i} \tag{10}$$

are the essential colonization rate of populations on a patch. The stability of Q_0 is determined by the signs of δ_i. Q_0 is stable if both δ_i are negative, and unstable otherwise. Note that $b_ik_{i0} = \bar{\beta}_i\alpha_im_iK_i(1-m_i/r_i)$ describes the colonization ability of species i in the absence of other species. The condition $\delta_i > 0$, or equivalently, $\bar{e}_i < \bar{\beta}_i\alpha_im_ik_{i0}$ implies that the patch colonization rate needs to be greater than the patch extinction rate in order for the metapopulation to persist, which is consistent with the condition obtained form the Levin's model.

4. **Boundary equilibria of the slow system.** A boundary equilibrium here refers to an equilibrium at which at least one of the coordinates is zero and others are in $[0, 1]$. For the slow system (9), the only possible boundary equilibrium lies on the p_1 and p_2 axes. On the p_i axis $(i = 1, 2)$, the nonzero coordinate p^*_{ij} of the equilibrium Q_{ij} $(j = 1, 2)$ satisfies

$$b_i(k_{i0} + k_{i1}p_i)(1 - p_i) - \bar{e_i} = 0. \tag{11}$$

Hence, if

$$\Delta_i = \theta_i^2 + 4b_ik_{i1}\delta_i \geq 0,$$

then

$$p^*_{i1} = \frac{\theta_i - \sqrt{\Delta_i}}{2b_ik_{i1}}, \quad p^*_{i2} = \frac{\theta_i + \sqrt{\Delta_i}}{2b_ik_{i1}},$$

where

$$\theta_i = b_i(k_{i1} - k_{i0}). \tag{12}$$

Note that equation (11) can be written as

$$b_i(k_{i0} + k_{i1}p_i) - \frac{\bar{e_i}}{1 - p_i} = 0.$$

If regarding the left side of the equation as a function of p_i, then $p_i = 1$ is an asymptote of the function, and hence we have $p^*_{ij} < 1$. There are three possibilities for the solutions:

Case C_{ia}: $\delta_i > 0$, or $\delta_i = 0$ but $\theta_i > 0$ (where δ_i and θ_i are respectively given in (10) and (12)). In this case, the equation (11) has a unique positive root p^*_{i2}, which corresponds to the unique equilibrium Q_{i2} on the positive p_i axis.

Case C_{ib}: $\delta_i < 0$, $\Delta_i \geq 0$, $\theta_i > 0$. In this case, the equation (11) has two positive roots (counting multiplicity) $p^*_{i1} \leq p^*_{i2}$, which correspond to two equilibria Q_{i1}, Q_{i2}, on the positive p_i axis.

Case C_{ic}: $\delta_i < 0$, $\theta_i < 0$, $\Delta_i \geq 0$ or $\Delta_i < 0$. In this case, there are no roots of (11) in $(0, 1]$. Therefore, there are no equilibria on the positive p_i axis.

We now discuss the stabilities of these possible equilibria.

4.1. **Stability of boundary equilibria on the p_1-axis.** At $Q_{1j}(j = 1, 2)$, the Jacobian matrix of the show system (9) is given by

$$J_1(Q_{1j}) = \begin{pmatrix} v_{11} & v_{12} & v_{13} \\ 0 & v_{22} & v_{23} \\ 0 & v_{32} & v_{33} \end{pmatrix},$$

where

$$\begin{aligned} v_{11} &= (-1)^{j+1} p^*_{1j} \sqrt{\Delta_1}, \\ v_{22} &= b_2 N_2^*(p^*_{1j})(1 - p^*_{1j}) - \bar{e}_2 - \sigma_{12} b_1 N_1^*(p^*_{1j}) p^*_{1j}, \\ v_{23} &= b_2 N_2^*(p^*_{1j})(1 - p^*_{1j}) + E_1, \\ v_{32} &= \sigma_{12} b_1 N_1^*(p^*_{1j}) p^*_{1j} + \sigma_{21} b_2 N_2^*(p^*_{1j}) p^*_{1j}, \\ v_{33} &= \sigma_{21} b_2 N_2^*(p^*_{1j}) p^*_{1j} - (E_1 + E_2). \end{aligned}$$

Here,

$$N_1^*(p^*_{1j}) = k_{10} + k_{11} p^*_{1j}, \quad N_2^*(p^*_{1j}) = k_{20},$$

and k_{ij} are given in (8). v_{12} and v_{13} are of no interests. From the expression of v_{11}, we can see that in the case where two distinct equilibria Q_{11}, Q_{12} exist, Q_{11} is always unstable. The local stability of Q_{12} depends on the signs of $A_1(p^*_{12})$ and $B_1(p^*_{12})$, where

$$A_1(p^*_{12}) = v_{22} + v_{33}, \quad B_1(p^*_{12}) = v_{23} v_{32} - v_{22} v_{33}.$$

A straight forward calculation yields

$$\begin{aligned} A_1(p^*_{12}) &= b_2 N_2^*(p^*_{12})[1 - (1 - \sigma_{21}) p^*_{12}] - \bar{e}_2 - \sigma_{12} b_1 N_1^*(p^*_{12}) p^*_{12} - E_1 - \bar{e}_2 - \varepsilon_{21}, \\ B_1(p^*_{12}) &= [b_2 N_2^*(p^*_{12})(1 - (1 - \sigma_{21}) p^*_{12}) - \bar{e}_2][\sigma_{12} b_1 N_1^*(p^*_{12}) p^*_{12} + E_1 + \bar{e}_2] \\ &\quad + \varepsilon_{21}[b_2 N_2^*(p^*_{12})(1 - p^*_{12}) - \sigma_{12} b_1 N_1^*(p^*_{12}) p^*_{12} - \bar{e}_2]. \end{aligned} \tag{13}$$

Note that if $A_1(p^*_{12}) \geq 0$, then $B_1(p^*_{12}) > 0$. Therefore, the boundary equilibrium Q_{12} is stable if $B_1(p^*_{12}) < 0$ and unstable if $B_1(p^*_{12}) > 0$. From the expression of $B_1(p^*_{12})$, a sufficient condition for the stability of Q_{12} can be obtained as

$$b_2 N_2^*(p^*_{12})[1 - (1 - \sigma_{21}) p^*_{12}] < \bar{e}_2, \tag{14}$$

or equivalently,

$$\delta_2 < b_2 N_2^*(p^*_{12})(1 - \sigma_{21}) p^*_{12}. \tag{15}$$

Therefore, Q_{12} is always stable if $\delta_2 < 0$. In pure migration competition (i.e. $\varepsilon_{12} = \varepsilon_{21} = 0$), the sufficient condition (15) is also a necessary condition for the stability of Q_{12}. In summary, we have the following result:

Result 1 The boundary equilibrium Q_{11} is a saddle point as long as it exists and Q_{12} is a saddle point if $B_1(p^*_{12}) > 0$ and a stable node if one of the inequalities (15), $\delta_2 < 0$ and $B_1(p^*_{12}) < 0$ holds.

Note that $b_2 N_2^*(p^*_{12}) = \bar{\beta}_2 \alpha_2 m_2 K_2 (1 - m_2/r_2)$ describes the colonization ability of species 2. As in [4], the condition (15) has a clear ecological interpretation. That is, species 2 cannot invade a region occupied by species 1 if p^*_{12} is large and the colonization ability of species 2 is weak. This implies that a successful invasion is

unlikely when the original resident species is common and the invading species is rare.

4.2. **Stability of boundary equilibria on the p_2-axis.** Similar to the equilibrium Q_{1j}, the Jacobian matrix of the slow system (9) at $Q_{2j}(j=1,2)$ reads

$$J_2(Q_{2j}) = \begin{pmatrix} w_{11} & 0 & w_{13} \\ w_{21} & w_{22} & w_{23} \\ w_{31} & 0 & w_{33} \end{pmatrix},$$

where

$$\begin{aligned} w_{11} &= b_1 N_1^*(p_{2j}^*)(1-p_{2j}^*) - \sigma_{21} b_2 N_2^*(p_{2j}^*) p_{2j}^* - \bar{e}_1, \\ w_{13} &= b_1 N_1^*(p_{2j}^*)(1-p_{2j}^*) + E_2, \\ w_{22} &= (-1)^{j+1} p_{2j}^* \sqrt{\Delta_2}, \\ w_{31} &= \sigma_{12} b_1 N_1^*(p_{2j}^*) p_{2j}^* + \sigma_{21} b_2 N_2^*(p_{2j}^*) p_{2j}^*, \\ w_{33} &= \sigma_{12} b_1 N_1^*(p_{2j}^*) p_{2j}^* - (E_1 + E_2). \end{aligned}$$

Here,

$$N_1^*(p_{2j}^*) = k_{10}, \quad N_2^*(p_{2j}^*) = k_{20} + k_{21} p_{2j}^*,$$

and k_{ij} are given in (8). w_{21} and w_{23} are of no interests. Due to the expression of w_{22}, Q_{21} is always unstable as long as it exists. ¿From the same analysis of the stability of Q_{12}, it follows that the equilibrium Q_{22} is stable if

$$\begin{aligned} B_2(p_{22}^*) &= w_{13} w_{31} - w_{11} w_{33} \\ &= [b_1 N_1^*(p_{22}^*)(1-(1-\sigma_{12}) p_{22}^*) - \bar{e}_1](\sigma_{21} b_2 N_2^*(p_{22}^*) p_{22}^* + E_2 + \bar{e}_1) \\ &\quad + \bar{\varepsilon}_{12}[b_1 N_1^*(p_{22}^*)(1-p_{22}^*) - \sigma_{21} b_2 N_2^*(p_{22}^*) p_{22}^* - \bar{e}_1] < 0. \end{aligned} \tag{16}$$

Therefore, we have the stability result for boundary equilibria on p_2-axis.

Result 2 The boundary equilibrium Q_{21} is a saddle point as long as it exists and Q_{22} is a saddle point if $B_2(p_{22}^*) > 0$ and a stable node if $B_2(p_{22}^*) < 0$.

The existence and stability results of boundary equilibria are summarized in Table 2.

TABLE 2. Existence and stability of boundary equilibria ($i=1,2$).

	Existence		Stability	
	Q_{i1}	Q_{i2}	Q_{i1}	Q_{i2}
C_{ia}	No	Yes	N/A	Stable if $B_i(p_{i2}^*) < 0$, unstable if $B_i(p_{i2}^*) > 0$
C_{ib}	Yes	Yes	Unstable	Stable if $B_i(p_{i2}^*) < 0$, unstable if $B_i(p_{i2}^*) > 0$
C_{ic}	No		N/A	

4.3. **Bifurcations of boundary equilibria in a special case.** In the case where only pure migration competition ($\varepsilon_{12} = \varepsilon_{21} = 0$) and pure extinction competition ($\sigma_{12} = \sigma_{21} = 1$) exist, the stability of Q_{i2} is determined by the sign of δ_j ($i \neq j$). Table 3 illustrates the existence and local stabilities of boundary equilibria in this special case. Some phase portraits of the slow system (9) in the three cases (C_{1a}-C_{2a}, C_{1b}-C_{2b} and C_{1c}-C_{2c} in Table 3) are shown in Figure 1, which demonstrates some global properties of these equilibria.

TABLE 3. The existence and stability of boundary equilibria in the special case.

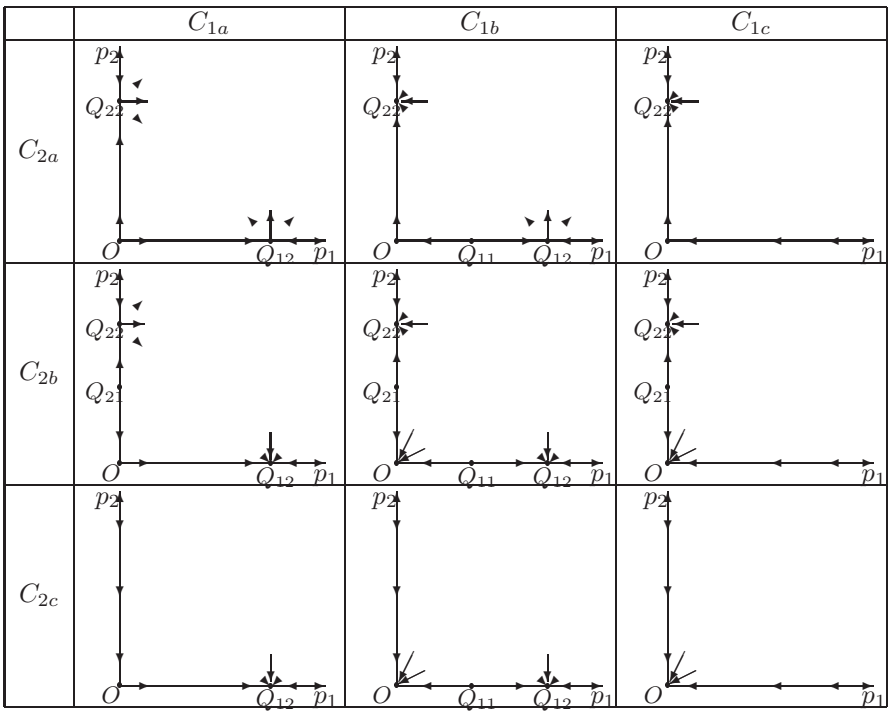

In [4], a simpler patch model is analyzed which does not include the local population changes explicitly. The unique positive equilibrium on each p_i-axis ($i = 1, 2$) is obtained and it is showed that if the competition effect of species reduces the colonization rate of the opposite species sufficiently, both boundary equilibria are stable and hence the outcome of regional competition depends on the initial abundance of the two species (priority effect). Priority effects exist in the slow system (9) as well. For example, in the case of C_{1b}-C_{2b} (see Table 3), three boundary equilibria Q_0, Q_{12} and Q_{22} are stable nodes, and hence the initial conditions determine where the solutions converge (see the middle panel in Figure 1). Priority effects are also present in model (3) ([2, 3]).

5. **Coexistence.** It is impossible to obtain analytical results for the slow system (9) for coexistence states (interior equilibria). However, some insights can be gained by studying the bifurcation of its boundary equilibria. Given a parameter space under consideration, the conditions listed in cases C_{ia} and C_{ib} provide the boundary of the region for the existence of the boundary equilibria Q_{i1} and/or Q_{i2} on the p_i

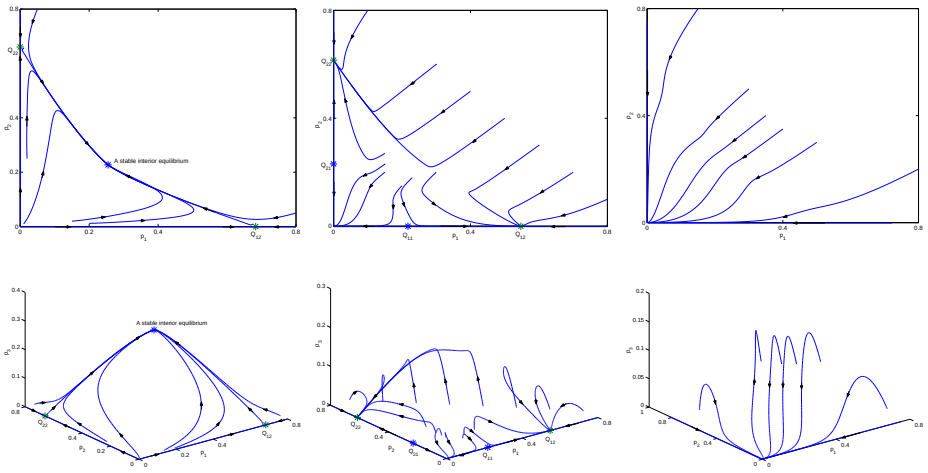

FIGURE 1. Typical phase portraits (in two and three dimensional phase spaces) of the slow system (9) in the cases of C_{1a}-C_{2a} (the left), C_{1b}-C_{2b} (the middle) and C_{1c}-C_{2c} (the right) in Table 3.

axis ($i = 1, 2$). The boundary equilibrium Q_{i1} is always unstable whenever it exists. Q_{i2} is stable if $B_i(p^*_{i2}) < 0$, where $B_i(p^*_{i2})$ are given by (13) and (16). If $B_i(p^*_{i2}) = 0$, then the Jacobian matrix of the slow system (9) at Q_{i2} has one zero and two nonzero eigenvalues. Therefore, a transcritical bifurcation occurs and hence an interior equilibrium may appear when parameter values vary and change the sign of $B_i(p^*_{i2})$.

For the bifurcation analysis in this section, we regard $\bar{e}_2$ and $\bar{\varepsilon}_{21}$ as bifurcation parameters for the slow system (9). From the conditions $\delta_2 < 0$ and $\Delta_2 > 0$ in the case C_{ib}, it follows that the boundary equilibria Q_{21} and Q_{22} exist if

$$b_2 k_{20} < \bar{e}_2 < \bar{e}_{2sn} = \frac{b_2}{4k_{21}}(k_{20} + k_{21})^2.$$

As the value of the parameter $\bar{e}_2$ decreases, Q_{21} moves toward the trivial equilibrium Q_0 along the p_2-axis, and coincides with the trivial equilibrium at $\bar{e}_2 = b_2 k_{20}$ (i.e., $\delta_2 = 0$). Therefore, when $\bar{e}_2 = b_2 k_{20}$, a transcritical bifurcation happens and the boundary equilibrium Q_{21} is bifurcated from the origin. For $\bar{e}_2 < b_2 k_{20}$, the equilibrium Q_{22} is the unique equilibrium on the positive p_2-axis (which falls into the case C_{ia}).

From the stability condition $B_2(p^*_{22}) < 0$ it follows that Q_{22} is stable if $\bar{\varepsilon}_{21} < \bar{\varepsilon}_{21tr1}(\bar{e}_2)$, where

$$\begin{aligned}\bar{\varepsilon}_{21tr1}(\bar{e}_2) = &- \bar{e}_2 - \bar{e}_1 - \sigma_{21} b_2 N_2(p^*_{22}) p^*_{22} \\ &- \bar{\varepsilon}_{12} \frac{b_1 N_1(p^*_{22})(1 - p^*_{22}) - \sigma_{21} b_2 N_2(p^*_{22}) p^*_{22} - \bar{e}_1}{b_1 N_1(p^*_{22})[1 - (1 - \sigma_{12}) p^*_{22}] - \bar{e}_1}.\end{aligned}$$

On the curve $\bar{\varepsilon}_{21} = \bar{\varepsilon}_{21tr1}(\bar{e}_2)$, $B_2(p^*_{22}) = 0$ and a transcritical bifurcation occurs, in which case an interior equilibrium bifurcates from the boundary equilibrium Q_{22} either for $\bar{\varepsilon}_{21} < \bar{\varepsilon}_{21tr1}(\bar{e}_2)$ or for $\bar{\varepsilon}_{21} > \bar{\varepsilon}_{21tr1}(\bar{e}_2)$. Similarly, from the stability

condition $B_1(p_{12}^*) < 0$ it follows that Q_{12} is stable if $\bar{\varepsilon}_{21} > \bar{\varepsilon}_{21tr2}(\bar{e}_2)$, where

$$\bar{\varepsilon}_{21tr2}(\bar{e}_2) = -\frac{[b_2N_2(p_{12}^*)(1-(1-\sigma_{21})p_{12}^*) - \bar{e}_2][\sigma_{12}b_1N_1(p_{12}^*)p_{12}^* + \bar{e}_1 + \bar{e}_2 + \bar{\varepsilon}_{12}]}{b_2N_2(p_{12}^*)(1-p_{12}^*) - \sigma_{12}b_1N_1(p_{12}^*)p_{12}^* - \bar{e}_2}.$$

Q_{12} loses its stability through a transcritical bifurcation when the parameter $\bar{\varepsilon}_{21}$ decreases and passes through the curve $\bar{\varepsilon}_{21} = \bar{\varepsilon}_{21tr2}(\bar{e}_2)$. These results are summarized below.

Result 3 In the parameter plane $(\bar{e}_2, \bar{\varepsilon}_{21})$, a transcritical bifurcation occurs along the following curves:

(i) $\bar{e}_2 = b_2k_{20}$. The equilibrium Q_{21} bifurcates from the origin for $b_2k_{20} < \bar{e}_2$. The equilibrium Q_{21} exists for $b_2k_{20} < \bar{e}_2 < \bar{e}_{2sn}$ while Q_{22} exists for $0 < \bar{e}_2 < \bar{e}_{2sn}$.

(ii) $\bar{\varepsilon}_{21} = \bar{\varepsilon}_{21tr1}(\bar{e}_2)$. An interior equilibrium is bifurcated from Q_{22}, which loses its stability for $\bar{\varepsilon}_{21} > \bar{\varepsilon}_{21tr1}(\bar{e}_2)$.

(iii) $\bar{\varepsilon}_{21} = \bar{\varepsilon}_{21tr2}(\bar{e}_2)$. An interior equilibrium is bifurcated from Q_{12}, which loses its stability for $\bar{\varepsilon}_{21} < \bar{\varepsilon}_{21tr2}(\bar{e}_2)$.

In Figure 2, the lines $\bar{e}_2 = \bar{e}_{2sn}$ and $\bar{e}_2 = b_2k_{20}$ are respectively illustrated as L_1 and L_2, which are vertical lines in the $\bar{e}_2$-$\bar{\varepsilon}_{21}$ plane. For parameter values in the domain between the lines L_1 and L_2, two boundary equilibria Q_{21} and Q_{22} exist while in the domain to the left side of L_2 only Q_{22} exists on the positive p_2-axis. In the figure, the curves C_1 and C_2 represent the curves $\bar{\varepsilon}_{21} = \bar{\varepsilon}_{21tr1}(\bar{e}_2)$ and $\bar{\varepsilon}_{21} = \bar{\varepsilon}_{21tr2}(\bar{e}_2)$, respectively. Thus, Q_{22} is stable when parameters are in the region below C_1 and unstable above the curve while the stable region for Q_{12} lies above C_2.

The curves C_1 and C_2 intersect and form two regions in the $\bar{e}_2$-$\bar{\varepsilon}_{21}$ plane: the region I, unstable region for both boundary equilibria Q_{12} and Q_{22}, and the region II where both equilibria are stable. Thus priority effect exists when parameters lie in the region II, that is, the initial population sizes of two species determine the outcome of the competition. In both regions I and II, interior equilibria are expected to exist due to transcritical bifurcations. The typical phase portraits for parameters in Regions I and II are illustrated in Figure 3.

To get more detailed information about coexistence states, we traced interior equilibria bifurcated from Q_{12} and Q_{22} using AUTO. In order to study the interior equilibria in the unstable region I as shown in Figure 2, we fix all parameters except $\bar{e}_2$. Figure 4 illustrates how interior equilibria of system (9) and their stabilities may vary with the parameter $\bar{e}_2$. Solid curves in the figure represent stable equilibria and dashed ones denote unstable equilibria. A branch of stable interior equilibria is bifurcated from Q_{12} when $\bar{e}_2$ decreases and crosses the curve C_2: $\bar{\varepsilon}_{21} = \bar{\varepsilon}_{21tr2}(\bar{e}_2)$ while another branch of unstable interior ones is bifurcated from Q_{22} as $\bar{e}_2$ decreasingly passes through the curve C_1: $\bar{\varepsilon}_{21} = \bar{\varepsilon}_{21tr1}(\bar{e}_2)$. These two branches of equilibria coincide with each other through a saddle-node bifurcation at a point lying below both C_1 and C_2 in the $\bar{e}_2$-$\bar{\varepsilon}_{21}$ plane. Thus, in the region I there is a stable coexistence state. To confirm and extend the bifurcation diagram shown in Figure 4 and to see how the stabilities of equilibria vary, we numerically computed solutions of the slow system (9) for different values of $\bar{e}_2$. Figure 5 shows that two solutions in the left panel converge to the boundary equilibrium Q_{22} when $\bar{e}_2 = 0.5$. As $\bar{e}_2$ increases, one of these two solutions goes to a stable interior equilibrium while the another one still goes to Q_{22} (see the middle panel in the figure). As $\bar{e}_2$ is further

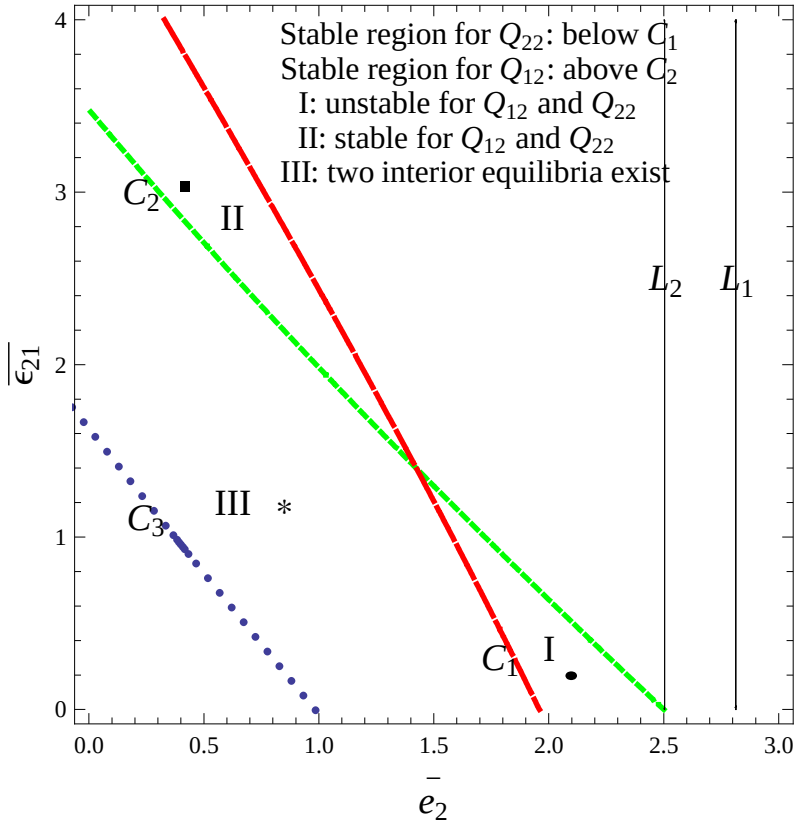

FIGURE 2. An example to illustrate the stability regions of boundary equilibria Q_{12} and Q_{22}. The stable region for Q_{22} lies below the curve C_1 while the region for Q_{12} lies above C_2. The curves C_1 and C_2 intersect and form two regions: the bi-unstable region I, the bi-stable region II. Q_{22} exists to the left of L_1 while Q_{21}, which is a saddle point, exists in the domain between L_1 and L_2. The curve C_3 represents the critical curve on which a saddle-node bifurcation of interior equilibria occurs (see text). In the region III enclosed by the curves C_1, C_2 and C_3, there are a stable and an unstable interior equilibria. Typical phase portraits of the slow system (9) in the regions I, II and III are shown in Figure 3. Here the parameters take the following values: $r_1 = 1, r_2 = 1.5, m_1 = 0.8, m_2 = 1, a_{12} = a_{21} = 0.5, \alpha_1 = \alpha_2 = 1, \bar{\beta}_1 = \bar{\beta}_2 = 0.05, K_1 = K_2 = 150, \sigma_{12} = \sigma_{21} = 1, \bar{e}_1 = 0.57, \bar{\varepsilon}_{12} = 1$.

increased, both solutions converge to the boundary equilibrium Q_{12} (see the right panel). These simulations are consistent with our bifurcation diagram.

It is worthwhile to notice that the saddle-node bifurcation of interior equilibria occurs at a point in the region where the boundary equilibrium Q_{22} is stable and Q_{12} is unstable. Therefore, when the stable coexistence state of two species is around the saddle-node bifurcation point (i.e., when $\bar{e}_2$ is near 0.86 in Figure 4), species 1 may suddenly disappear regionally and only species 2 exists in the landscape

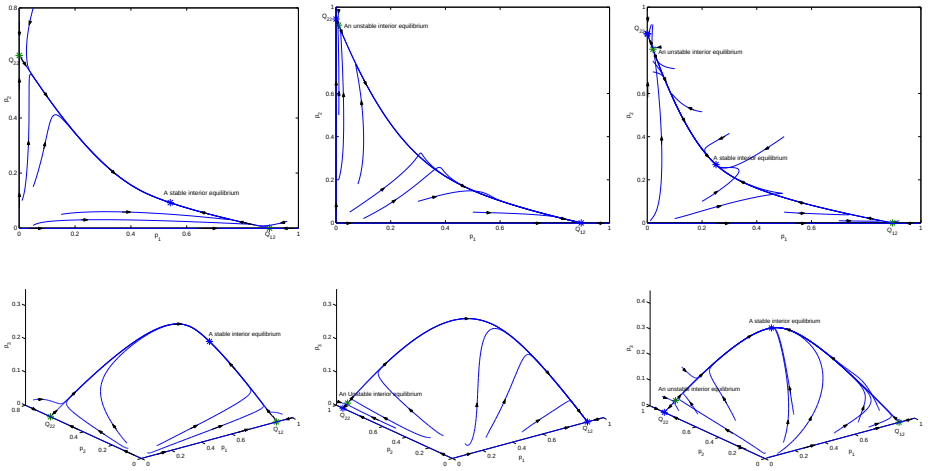

FIGURE 3. The phase portraits (in two- and three-dimensional spaces) of the slow system (9) when $(\bar{e}_2, \bar{\varepsilon}_{21}) = (2.1, 0.2)$ (the left), $(0.85, 1.2)$ (the middle) and $(0.4, 3)$ (the right), respectively corresponding to the disc in Region I, the rectangle in Region II and the star in Region III shown in Figure 2. Other parameters take the same values as in Figure 2.

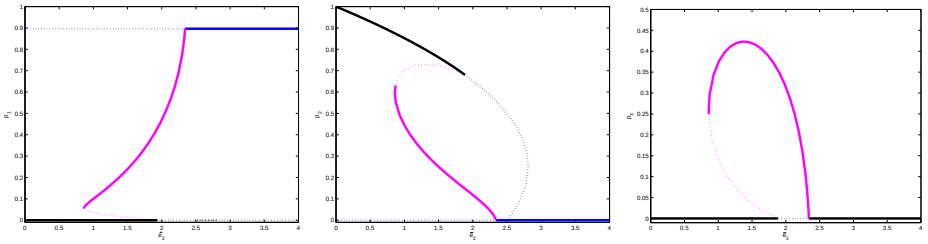

FIGURE 4. An example to show the transcritical bifurcations occurring at boundary equilibria Q_{12} and Q_{22} as the parameter $\bar{e}_2$ varies. Here $\bar{\varepsilon}_{21}$ is set to be 0.2 to investigate interior equilibria in the region I. Other parameters take the same values as in Figure 2.

if parameter values are slightly changed. This is important especially from the viewpoint of conservation. It is necessary to determine the critical boundary in the $\bar{e}_2$-$\bar{\varepsilon}_{21}$ plane where a saddle-node bifurcation occurs. Using AUTO, we traced the saddle-node bifurcation point of interior equilibria when both $\bar{e}_2$ and $\bar{\varepsilon}_{21}$ vary. The critical boundary on which a saddle-node bifurcation occurs is shown as a dotted curve C_3 in Figure 2. Therefore, in the region (III) enclosed by the curves C_1, C_2 and C_3 there are two interior equilibria (stable and unstable). A typical phase portrait of the system in the region III is shown in the right panel of Figure 3. Since Q_{22} is also stable in the region III, priority effect exists and the outcome of the competition may be coexistence or species 2 only.

We regard $\bar{\varepsilon}_{21}$ as the bifurcation parameter and fix all other parameters to study interior equilibria in the bistable region II for the boundary equilibria Q_{12} and Q_{22}.

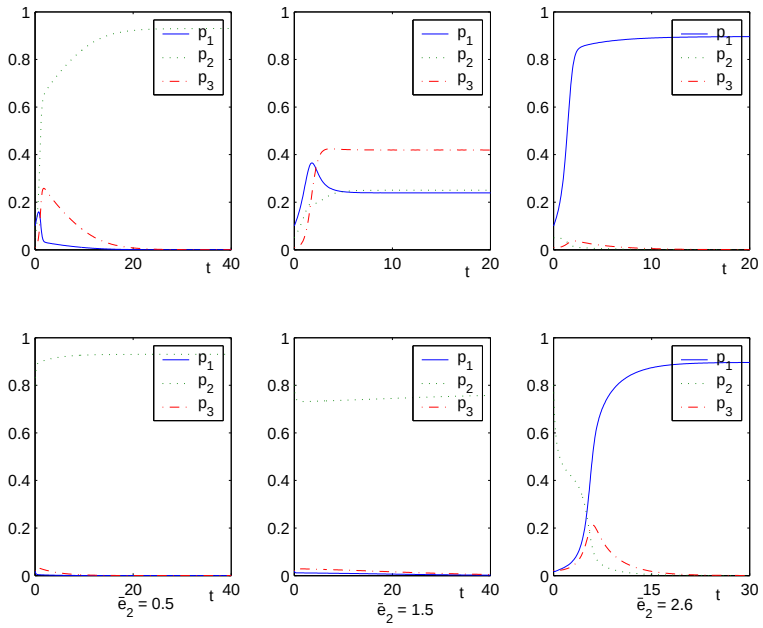

FIGURE 5. The time plots of two solutions of the slow system (9) for different values of $\bar{e}_2$. In the left panel where $\bar{e}_2 = 0.5$, both solutions converge to the boundary equilibrium Q_{22}. In the middle panel where $\bar{e}_2 = 1.5$, one of these two solutions goes to an interior equilibrium and another one still converges to Q_{22}. In the right panel where $\bar{e}_2 = 2.6$, both solutions converge to the boundary equilibrium Q_{12}. These results are consistent with the bifurcation diagram Figure 4. All parameters except $\bar{e}_2$ take the same values as in Figure 4.

Figure 6 shows the bifurcation diagram as the parameter $\bar{\varepsilon}_{21}$ varies while in Figure 7 two solutions of the slow system (9) are plotted for different values of $\bar{\varepsilon}_{21}$. The diagram in Figure 6 is a little different from the one in Figure 4. An unstable interior equilibria is bifurcated from Q_{12} as $\bar{\varepsilon}_{21}$ increasingly passes through a critical value (on the curve C_2). When $\bar{\varepsilon}_{21}$ is slightly greater than the critical value, the branch of unstable interior equilibria gains its stability through a saddle-node bifurcation point, whose corresponding values of $\bar{e}_2$ and $\bar{\varepsilon}_{21}$ lie in the bistable region II. After the branch of unstable equilibria becomes stable, it meets with the branch of unstable ones bifurcated from Q_{22} as $\bar{\varepsilon}_{21}$ decreases and crosses the saddle-node bifurcation curve C_3 (in Figure 2). Therefore, in the bistable region II, there is a small region near the curve C_2, where three interior equilibria exist (with one being stable and the other two unstable). Away from the above mentioned small region in the region II, system (9) has two stable boundary and one unstable equilibria. Therefore, in the bistable region II, two species are unlikely to coexist.

We summarize the existence and stability of equilibria of the slow system (9) in Table 4. In short, we can conclude that either two species are expected to coexist or only species 2 exists in region III (where priority effect exists) and two species coexist in region I. In the most part of the bistable region II, only one species exists

regionally (priority effect determines which species exists) while in a small region of II there may be species 1 only, or species 2 only, or both species regionally (priority effect determines the final state).

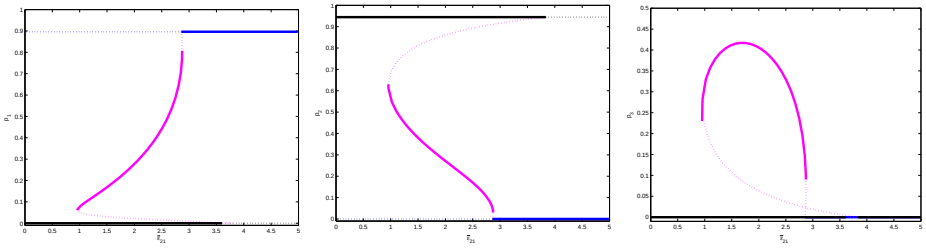

FIGURE 6. An example to show the transcritical bifurcations occurring at boundary equilibria Q_{12} and Q_{22} regarding $\bar{\varepsilon}_{21}$ as the bifurcation parameter. Here $\bar{e}_2$ is set to be 0.4 to study interior equilibria in the bistable region II. Other parameters values are the same as in Figure 2.

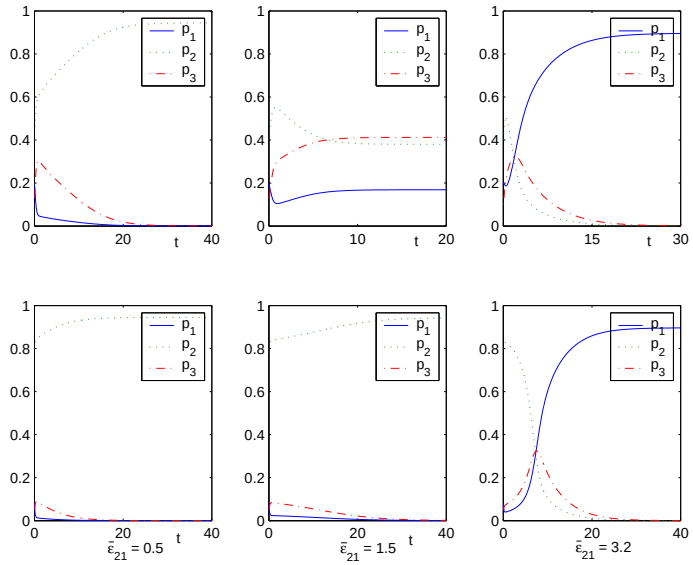

FIGURE 7. The time plots of two solutions of the slow system (9) for different values of $\bar{\varepsilon}_{21}$. In the left panel where $\bar{\varepsilon}_{21} = 0.5$, both solutions converge to the boundary equilibrium Q_{22}. In the middle panel where $\bar{\varepsilon}_{21} = 1.5$, one of these two solutions goes to an interior equilibrium and another one still converges to Q_{22}. In the right panel where $\bar{\varepsilon}_{21} = 3.2$, both solutions converge to the boundary equilibrium Q_{12}. These results are consistent with the bifurcation diagram Figure 6. All parameters except $\bar{\varepsilon}_{21}$ take the same values as in Figure 6.

TABLE 4. Existence and stability of equilibria for system (9).

Region in Figure 2	Interior equilibria	Q_{12}	Q_{22}
I	One, stable	Unstable	Unstable
II	At least one, unstable	Stable	Stable
III	One stable and one unstable	Unstable	Stable

6. **Discussion.** We generalized the mean-field competitive metapopulation model (3) studied in [2, 3] by including a more detailed description of the model with regard to singly and doubly occupied patches. The generalized model inherits the main characteristics of the original model, i.e., the presence of multiple coexistence states. Our bifurcation analysis shows that as parameter values vary, the current model may display dramatically different dynamics including only one stable coexistence state (the region I), one stable and two unstable coexistence states (a small region in the region II), bistability (one stable boundary equilibrium and one stable coexistence state in the region III) and tri-stability (two stable boundary and one stable interior equilibria, e.g., in the region II). The boundary equilibria Q_{12} and Q_{22} of the slow system (9) are either stable nodes or saddle points and hence they always have stable manifolds. Thus, even if both Q_{12} and Q_{22} are unstable (e.g., in the region I), stable interior equilibria can not be globally stable and the system (9) cannot have uniform persistence. Therefore priority effect always exists due to competitions. This illustrates a main difference in model outcomes comparing with model (3), which is resulted from the inclusion of the doubly occupied patches, p_3.

The existence of the equilibria Q_{ij} on the positive p_i axis is determined by the intrinsic colonization rate δ_i of species i, and hence, it depends on the balance between the colonization rate at the trivial equilibrium Q_0 and the extinction rate. Therefore, our model inherits the main characteristics of Levins' model.

The slow system (9) is formally the same as Slatkin's model [19] and its variations in [4, 18, 21] except that parameters of the local dynamics are included. Therefore, the model (4) and the system (9) are generalizations of these simple patch models, and the effects of the local dynamics on the regional dynamics can be examined by studying system (9) in the same way as done in the last section. Compared with the simple patch models, model (4) generates much richer dynamics including bistability and multiple interior equilibria. It also inherits some of the results obtained from patch models such as those in [4]. The condition (15) for the stability of Q_{12} is formally similar to the condition (5) in [4] except the parameters used to describe the local dynamics, and hence, it generates the similar biological explanations.

REFERENCES

[1] Y. DeWoody, Z. Feng and R. Swihart, *Merging spatial and temporal structure within a metapopulation model*, American Naturalist, **66** (2005), 42–55.

[2] Z. Feng, Y. Yi and H. Zhu, *Metapopulation dynamics with migration and local competition*, Fields Inst. Commun., **36** (2003), 119–135.

[3] Z. Feng, R. Swihart, Y. Yi and H. Zhu, *Coexistence in a metapopulaiton model with explicit local dynamics*, Math. Biosci. Engi., **1** (2004), 131–145.

[4] I. Hanski, *Coexistence of competitors in patchy environment*, Ecology, **64** (1983), 493–500.

[5] I. Hanski, *Single species spatial dynamics may contribute to long term rarity and commonness*, Ecology, **66** (1985), 335–343.

[6] I. Hanski and D. Zhang, *Migration, metapopulation dynamics and fugitive coexistence*, J. Theor. Biol., **163** (1993), 491–504.

[7] I. Hanski and M. Gyllenberg, *Uniting two general patterns in the distribution of species*, Science, **275** (1997), 397–400.
[8] I. Hanski, "Metapopulation Ecology," Oxford University Press, 1999.
[9] I. Hanski and O. Ovaskainen, *The metapopulation capacity of a fragmented landscape*, Nature, **404** (2000), 755–758.
[10] I. Hanski and O. Ovaskainen, *Metapopulation theory for fragmented landscapes*, Theor. Popul. Biol., **64** (2003), 119–127.
[11] J E. Keymer, P A. Marquet, J X. Velasco-Hernández and S A. Levin, *Extinction thresholds and metapopulation persistence in dynamic landscapes*, The American Naturalist, **156** (2000), 478–494.
[12] C A. Klausmeier, *Habitat destruction and extinction in competitive and mutualistic metacommunities*, Ecol. Lett., **4** (2001), 57–63.
[13] R. Levins, *Some demographic and genetic consequences of environmental hetereogeneity for biological control*, Bulletin of the Entomological Society of America, **15** (1969), 237–240.
[14] R. Levins, *Extinction*, Lecture Notes in Mathematics, **2** (1970), 75–107.
[15] S. Nee and R. May, *Dynamics of metapopulations: Habitat destruction and competitive coexistence*, J. Ani. Ecol., **61** (1992), 37–40.
[16] S. Nee, R. May and M. Hassell, *Two-species metapopulation models*, in "Metapopulation Biology: Ecology, Genetics and Evolution" (eds. I. Hanski and M. Gilpin), Academic Press, (1997), 123–147.
[17] S. Prakash and A M. de Roos, *Habitat destruction in a simple predator-prey patch model: How predators help prey to persist*, Theor. Popul. Biol., **62** (2002), 231–249.
[18] S. Prakash and A M. de Roos, *Habitat destruction in mutualistic metacommunities*, Theor. Popul. Biol., **65** (2004), 153–163.
[19] M. Slatkin, *Competition and regional coexistence*, Ecology, **55** (1974), 128–134.
[20] R. Swihart, Z. Feng, N S. Slade, D M. Doran and T M. Gehring, *Effects of habitat destruction and resource supplementation in a predator-prey metapopulation model*, J. Theor. Biol., **210** (2001), 287–303.
[21] D E. Taneyhill, *Metapopulation dynamics of multiple species: The geometry of competition in a fragmented habitat*, Ecological Monographs, **70(4)** (2000), 495–516.
[22] D. Xu, Z. Feng, L. Allen and R. Swihart, *A spatially structured metapopulation model with patch dynamics*, J. Theor. Biol., **239** (2006), 469–481.

Received September 2008; revised April 2009.

E-mail address: dxu@math.siu.edu
E-mail address: zfeng@math.purdue.edu